Crossover Behavior in High-Frequency Dielectric Relaxation of Linear Polyions in Dilute and Semidilute Solutions

Kohzo Ito,*,† Akira Yagi, Norio Ookubo, and Reinosuke Hayakawa

Department of Applied Physics, Faculty of Engineering, University of Tokyo, Bunkyo-ku, Tokyo 113, Japan. *Received February 23, 1989; Revised Manuscript Received June 29, 1989*

ABSTRACT: The complex dielectric constant, ϵ^*, of the high-frequency dielectric relaxation of sodium polystyrene sulfonate (NaPSS) in aqueous solutions with no added salts was measured over wide ranges of degree of polymerization, N, and polymer concentration, C_P, from the dilute to the semidilute region. The crossover concentration, C_G, between the dilute and the semidilute regions was clearly observed in the C_P dependences of the relaxation time, τ, and the dielectric increment, $\Delta\epsilon$, of the high-frequency relaxation. The C_P and N dependences of τ and $\Delta\epsilon$ are summarized as $\tau \propto C_P^{-2/3}N^{2/3}$, $\Delta\epsilon \propto C_P^{1/3}N^{2/3}$ below C_G, and $\tau \propto C_P^{-1}N^0$, $\Delta\epsilon \propto C_P^0N^0$ above C_G. This crossover behavior of the high-frequency relaxation is ascribable to that of the correlation length, ξ, which shows different C_P dependences in the dilute and semidilute regions, respectively. This leads to the conclusion that the high-frequency relaxations in the dilute and semidilute regions are commonly attributed to the localized movement or fluctuation of loosely bound counterions spreading over ξ, namely, the average distance between polyions in both the regions.

Introduction

A highly charged linear polyion in the dilute solution with no added salts has an extended, rodlike conformation due to the Coulombic repulsion between dissociated groups on the polyion. As the polymer concentration C_P increases, there occurs a crossover from the dilute region to the semidilute one where the polyions of rodlike or semiflexible conformation are entangled with each other. Part of counterions in the semidilute region are known to be bound to the polyion by a Coulombic attraction from the polyion which consequently loses its activity. This is the counterion condensation phenomenon,[1,2] typical in the semidilute region. The solution of linear polyions in the semidilute region is thus regarded as a Coulombic many-body system where a crowd of linearly charged polyions surrounded by the bound counterions are randomly dispersed in the aqueous medium.

The dielectric relaxation spectroscopy for measuring the complex dielectric constant, ϵ^*, as a function of frequency directly reflects the dynamic properties of the polyion–counterion system, highly sensitive to electrical stimulus, and is expected to give us useful information on the details of the Coulombic interaction between the bound counterions and the polyion in the solution.[1,3] Such information is not obtainable from the usual static measurements used to determine dc conductivity, osmotic pressure, and so on.

It is well-known that dielectric relaxation spectroscopy for the linear polyions in the semidilute region shows two kinds of relaxation processes, i.e. the low-frequency and high-frequency ones. The former strongly depends on the degree of polymerization, N, or the molecular weight M_w of a polyion[4-9] while the latter is nearly independent of N.[10,11] The N dependence of the low-frequency relaxation indicates that this relaxation is ascribable to the fluctuation of the bound counterions along the polyion axis.[1,3]

On the other hand, the molecular mechanism for the high-frequency relaxation has long been controversial. The mechanisms proposed so far are the Maxwell–Wagner effect,[10] the bound counterion fluctuation along the polyion within the range of the correlation length, ξ,[3,12] and the bound counterion fluctuation perpendicular to the polyion axis.[1,13-16] The correlation length, ξ, is the parameter that characterizes the concentration regions of the polyion solution[12] and is identified with the average distance between polyions both in the dilute and semidilute regions in the case of no added salts. Incidentally, the C_P dependence of ξ is given by $\xi \propto C_P^{-1/3}$ and $\xi \propto C_P^{-1/2}$ in the dilute and semidilute regions, respectively.

The frequency-domain electric birefringence (FEB) spectroscopy has been recently developed and applied to the linear polyion solutions in the semidilute region.[17] This technique enables us to obtain information on the dielectric anisotropy, i.e., on the direction of electric polarization which contributes to each relaxation process. The FEB result for sodium polystyrene sulfonate (NaPSS) in the semidilute solution has shown that the direction of the polarization in the high-frequency relaxation is perpendicular to that in the low-frequency one. This clearly indicates that the high-frequency relaxation in the semidilute region is ascribable to the counterion fluctuation in the direction perpendicular to the polyion axis, namely, the interpolyion direction.

This type of interpolyion fluctuation of bound counterions is expected to be observed in the dilute region as well as in the semidilute one. The purpose of the present paper is to obtain a detailed picture of the high-frequency dynamics of the bound counterions in the polyion solution by measuring ϵ^* of aqueous NaPSS with different N over a wide C_P range from the dilute to the semidilute region.

Experimental Section

The NaPSS samples used in this measurement are listed in Table I. Seven kinds of monodisperse NaPSS samples with different N were purchased from Pressure Chemical Co. The NaPSS solutions were all dialyzed against freshly deionized water, passed through a mixed-bed ion-exchange column, neutralized by adding a freshly prepared NaOH solution, and used after dilution with pure water.

The ϵ^* measurement in the high-frequency range of 1 MHz to 1 GHz was carried out by using the RF impedance analyzer (HP 4191A). The specimen cell used was a coaxial type of cylindrical condenser with platinum-plated stainless steel electrodes. We performed the comparative measurements between

* Correspondence should be sent to K. Ito, Ph.D.
† Present address: Research Institute for Polymers and Textiles, 1-1-4 Higashi, Tsukuba, Ibaraki 305, Japan.

0024-9297/90/2223-0857$02.50/0

Table I
Degree of Polymerization (N) of NaPSS Samples Used in the Present Measurement

samples	N
P1	3800
P2	2000
P3	1000
P4	500
P5	350
P6	170
P7	87

the polyion solution and the KCl one with the same conductivity as the polyion solution to eliminate the influence of residual resistance between the cell and the test port of the impedance analyzer.

On the other hand, the measurements below 1 MHz were carried out by the multifrequency simultaneous measurement technique using a sum of sinusoidal waves with a geometrical frequency series of the common ratio 2. The cell used in the measurements was a parallel-plate condenser type with black-platinized platinum electrodes. The outline of this technique was described in previous papers.[18-20]

The C_P range of the polymer solutions was 0.05–60 g/L, which covered dilute and semidilute regions. All the measurements of ϵ^* were performed at 20.0 ± 0.1 °C.

Results

As a typical example of the results, Figure 1a shows the complex dielectric constant $\epsilon^* = \epsilon' - i\epsilon''$ of a solution of NaPSS of the sample P3 with C_P = 0.4 g/L, where the contributions of both the dc conductivity, $\sigma(0)$, and the dielectric constant, ϵ_S, of the solvent have been subtracted. The Cole–Cole plot obtained from the data in Figure 1a is given as Figure 1b. In parts a and b of Figure 1, closed circles represent the observed data points and the solid curves are the best fitting ones obtained by an iterative type of nonlinear least-squares method with the semiempirical formula of Havriliak–Negami:[21]

$$\epsilon^* = \frac{\Delta\epsilon_L}{[1 + (i\omega\tau_L')^{\beta_L}]^{\alpha_L}} + \frac{\Delta\epsilon}{[1 + (i\omega\tau')^{\beta}]^{\alpha}} + \frac{\sigma(0)}{i\omega\epsilon_0} + \epsilon(\infty) \quad (1)$$

where ϵ_0 is the vacuum permittivity equal to 8.854×10^{-12} F/m and $\epsilon(\infty)$ is the high-frequency limit of ϵ^*. The first and second terms on the right-hand side of eq 1 correspond to the low-frequency and high-frequency relaxations, respectively. In these terms, $\Delta\epsilon$ is the dielectric increment and τ' is the nominal relaxation time. The average relaxation time, τ, is calculated from the peak frequency, f_m, of ϵ'' in each relaxation as $\tau = 1/(2\pi f_m)$. The parameters α and β represent asymmetry and broadness in the distribution of relaxation times. The suffix L in eq 1 stands for the low-frequency relaxation, while no suffix means the high-frequency relaxation. Parts a and b of Figure 1 indicate that the observed data are in a good agreement with the best fitting curves using eq 1, which give us the optimum values of relaxation parameters $\Delta\epsilon$, τ, α, and β.

The high-frequency relaxation data and the best fitting curves are shown in Figure 2 over a C_P range of 0.05–29 g/L for the sample P2. The figure indicates that the peak frequency, f_m, increases with increasing C_P while the dielectric increment $\Delta\epsilon$ is nearly independent of C_P for a wide range of C_P's, i.e., from 0.05 to 29 g/L.

As shown in parts a and b of Figure 3, the C_P dependences of τ and $\Delta\epsilon$ of the samples P3, P4, P5, and P6 have a slope change at some concentration C_G that is different for each sample. This turning point concentration, C_G, which decreases with increasing degree of poly-

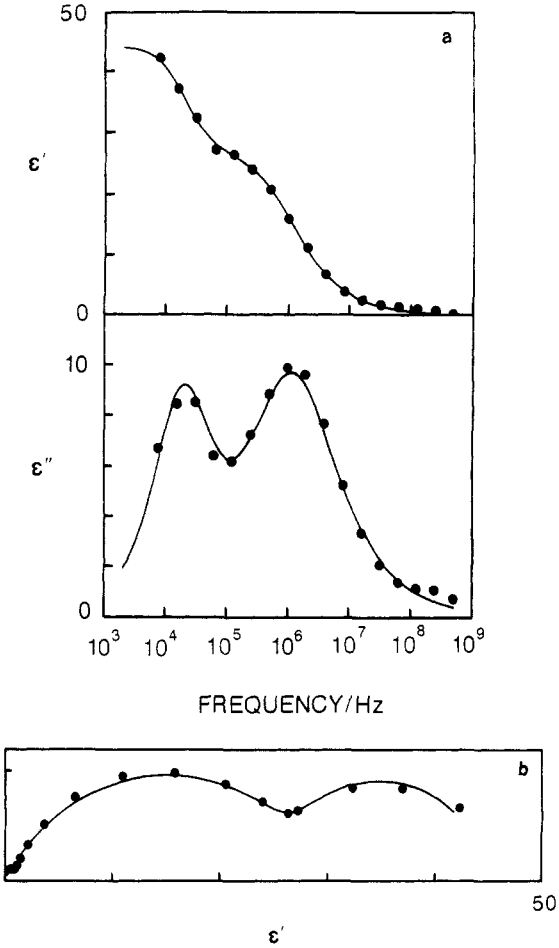

Figure 1. (a) Real part, ϵ', and imaginary part, ϵ'', of the complex dielectric constant, ϵ^*, of a NaPSS solution of the sample P3 with C_P = 0.4 g/L. (b) Cole–Cole plot obtained from the data in Figure 1a. In both the figures, the closed circles represent the observed data points and the solid curves are the best fitting ones by eq 1.

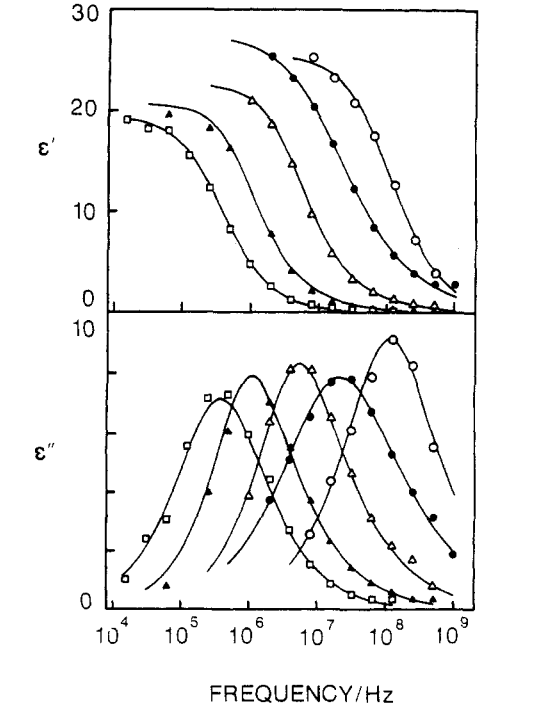

Figure 2. High-frequency relaxation data of ϵ' and ϵ'' for the sample P2. Each symbol represents C_P: □, 0.05 g/L; ▲, 0.2 g/L; △, 1 g/L; ●, 4 g/L; ○, 29 g/L. The solid curves are the best fitting ones by eq 1.

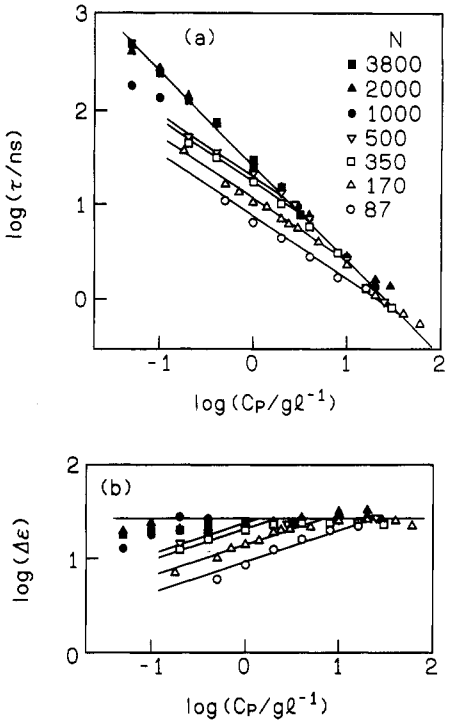

Figure 3. (a) Doubly logarithmic plot of τ against C_P; the solid straight lines have a slope of −1 or −2/3. (b) Doubly logarithmic plot of $\Delta\epsilon$ against C_P; the solid straight lines have a slope of 0 or 1/3. In both the figures, each symbol represents a sample difference: ■, P1; ▲, P2; ●, P3; ▽, P4; □, P5; △, P6; ○, P7.

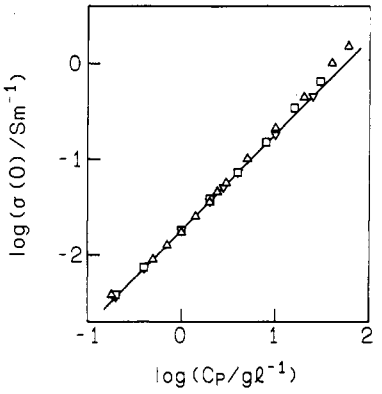

Figure 4. Doubly logarithmic plot of $\sigma(0)$ against C_P. Each symbol represents the sample difference as in Figure 3; the solid straight line has a slope of unity.

merization, N, can be identified with the crossover concentration from the dilute region to the semidilute one. As extreme examples, the samples P1 and P2 with the largest N always belong to the semidilute one while the sample P7 with the smallest N always belongs to the dilute one. The C_P dependences of τ and $\Delta\epsilon$ for all the samples in Figure 3 are summarized as $\tau \propto C_P^{-2/3}$, $\Delta\epsilon \propto C_P^{1/3}$, for the dilute region and $\tau \propto C_P^{-1}$, $\Delta\epsilon \propto C_P^{0}$, for the semidilute one, respectively. The dependence for the semidilute region is not in agreement with that obtained by van der Touw and Mandel.[11]

The N dependences of τ and $\Delta\epsilon$ are found only in the dilute region and not in the semidilute one, as seen in parts a and b of Figure 3. Incidentally, the parameters α and β for the high-frequency relaxation were nearly unity ($\alpha \geq 0.95$ and $\beta \geq 0.9$) for all the solutions of NaPSS, which indicates that the high-frequency relaxation process is close to Debye type.

Figure 4 shows that the dc conductivity, $\sigma(0)$, increases

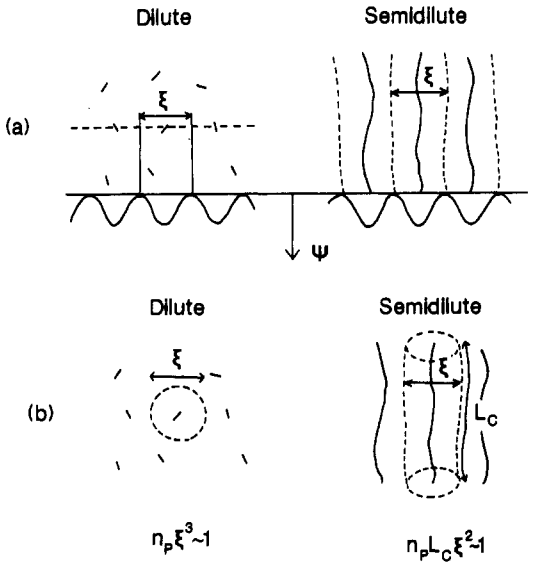

Figure 5. Polyions distributed with the average distance or the correlation length, ξ, in the dilute and semidilute regions. (a) The profiles of the electrostatic potential, Ψ, in both regions are considered to have an approximate periodicity of ξ. (b) The cell models with the spherical free volume in the dilute region and with the cylindrical free volume in the semidilute one where n_P is the number concentration of polyions and L_c the polyion contour length.

linearly with C_P for samples P4, P5, and P6 and that the crossover behavior found in Figure 3 is not observed in $\sigma(0)$.

Discussion

As mentioned in the Introduction, the FEB result shows that the high-frequency relaxation in the semidilute region is ascribable to the counterion fluctuation in the direction perpendicular to the polyion axis. The present results of the dielectric measurements indicate that τ has a strong C_P dependence in both the dilute and semidilute regions, which cannot be explained by the independent contribution from the isolated polyions. In other words, we have to take into account the interpolyion interaction in the high-frequency relaxation process. We will then discuss the electric potential profile between polyions.

Figure 5a schematically shows the dilute and semidilute regions with no added salts where the polyions are distributed in solution with the average distance equal to the correlation length, ξ. To consider the electric potential exerted on counterions in such systems, we can use the cell model,[22] which assumes, for each polyion, a spherical free volume in the dilute region or a cylindrical one in the semidilute region with a diameter equal to the average distance between polyions as shown in Figure 5b. The electric potential calculated from the cell model (or free-volume model) in both the dilute and semidilute regions should have an approximate periodicity of ξ as shown in Figure 5a; in fact, the theoretical results for the semidilute region predict a spatial profile of the potential strongly dependent on ξ.[22] The bound counterions producing the high-frequency relaxation move or fluctuate in such an electric potential affected by the interaction between polyions.

The recent theoretical calculations based on the Poisson–Boltzmann (PB) equation have shown[23,24] that the bound counterions in the semidilute region are classified into two groups: the tightly bound counterions in the closest vicinity to the polyion and the loosely bound ones distributed around the tightly bound ones. On the other

hand, it is expected that there exist loosely bound counterions also in the dilute region, though a theoretical calculation has not been carried out because of the difficulty imposed by the boundary conditions. Now the question is which one of the two groups of bound counterions contributes to the high-frequency relaxation.

The tightly bound counterions are densely distributed around the polyion within a narrow range of the same order as the polyion radius and are trapped in a strong electric potential due to the charges of the dissociated groups on the polyion. The distribution of the tightly bound counterions in the semidilute region is nearly independent of C_P because they are hardly affected by the ionic atmosphere arising from the other groups of counterions (i.e., the loosely bound counterions and free counterions) whose concentration is proportional to C_P.[23,24]

The loosely bound counterions, on the other hand, are sparsely dispersed in a shallow electrostatic potential, Ψ, which has a depth on the order of thermal energy kT, owing to the shielding effect of the tightly bound counterions on the polyion charges, and has an approximate periodicity of ξ, as shown in Figure 5a. The loosely bound counterions in such a shallow potential valley (basins or troughs) can move locally or fluctuate within the range of ξ and would cause the polarizability in the direction perpendicular to the polyion axis in the semidilute region. Since ξ depends on C_P, the polarizability due to the loosely bound counterions should have a strong C_P dependence in its magnitude and relaxational behavior. The present experimental result that τ has a strong C_P dependence in both the dilute and semidilute regions suggests that the high-frequency relaxation is ascribable to the localized movement or fluctuation of the loosely bound counterions within the range of ξ.

Now we estimate the C_P dependence of τ from that of ξ in both of the two regions. In the case of the dielectric relaxation due to the counterion fluctuation within the range of ξ, τ is given by

$$\tau \sim \xi^2/2D \propto \xi^2 \tag{2}$$

where D is the diffusion constant of counterions.

Through a simple geometrical consideration based on the cell models for the dilute and semidilute regions as shown in Figure 5b, we obtain the C_P and N dependences of ξ in both regions as

$$\xi \simeq n_P^{-1/3} \propto C_P^{-1/3}N^{1/3} \quad \text{dilute} \tag{3}$$

$$\xi \simeq (n_P L_c)^{-1/2} \propto C_P^{-1/2}N^0 \quad \text{semidilute} \tag{4}$$

where n_P is the number concentration of polyions and L_c the polyion contour length. By substituting ξ in eq 3 and 4 into eq 2, we obtain the C_P and N dependences of τ as

$$\tau \propto C_P^{-2/3}N^{2/3} \quad \text{dilute} \tag{5}$$

$$\tau \propto C_P^{-1}N^0 \quad \text{semidilute} \tag{6}$$

These dependences in the dilute and semidilute regions agree well with the experimental results, as shown by solid lines in Figure 3a.

The dielectric increment, $\Delta\epsilon$, on the other hand, can be estimated for the mechanism of the counterion fluctuation as follows. The electrical polarizability α_e due to a loosely bound counterion is given by

$$\alpha_e = \langle\mu^2\rangle/kT \tag{7}$$

where $\langle\mu^2\rangle$ is the mean-square fluctuation of dipole moment, μ, produced by the counterion. The dielectric increment, $\Delta\epsilon$, is expressed in terms of α_e as

$$\Delta\epsilon = n_L\alpha_e/\epsilon_0 \tag{8}$$

where n_L is the number concentration of the loosely bound counterions. Introducting eq 7 into eq 8, we have

$$\Delta\epsilon = n_L\langle\mu^2\rangle/(\epsilon_0 kT) \tag{9}$$

Since the loosely bound counterion fluctuates within the range of ξ, $\langle\mu^2\rangle$ is estimated as

$$\langle\mu^2\rangle \sim e^2\xi^2 \tag{10}$$

where e is the elementary charge. Substitution of eq 10 into eq 9 yields

$$\Delta\epsilon \sim n_L e^2\xi^2/(\epsilon_0 kT) \propto n_L\xi^2 \tag{11}$$

Theoretical calculations[23,24] have shown that n_L is proportional to C_P in the semidilute region. From eq 2 and 11, we have an expression for n_L as

$$n_L \propto \epsilon_0\Delta\epsilon/\tau \tag{12}$$

Figure 6 shows $\epsilon_0\Delta\epsilon/\tau$ calculated from the observed τ and $\Delta\epsilon$, which indicates that n_L is proportional to C_P and independent of N in the dilute region as well as in the semidilute region. Then, the C_P and N dependences of $\Delta\epsilon$ are obtained from eq 11, 3, and 4 as

$$\Delta\epsilon \propto C_P^{1/3}N^{2/3} \quad \text{dilute} \tag{13}$$

$$\Delta\epsilon \propto C_P^0N^0 \quad \text{semidilute} \tag{14}$$

which agree well with the experimental results, as shown by solid lines in Figure 3b.

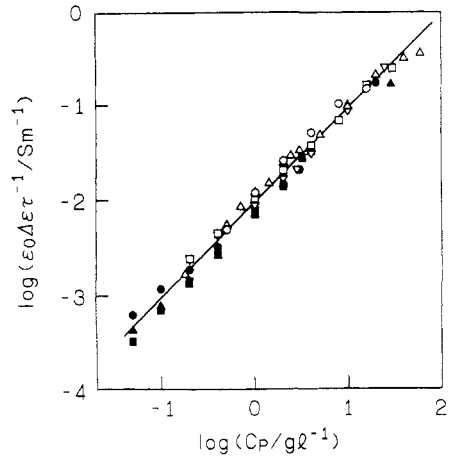

Figure 6. Doubly logarithmic plot of $\epsilon_0\Delta\epsilon/\tau$ against C_P. Each symbol represents the sample difference as in Figure 3; the solid straight line has a slope of unity.

To demonstrate the N dependence of τ and $\Delta\epsilon$ more clearly, parts a and b of Figure 3 are replotted as parts a and b of Figure 7 by using reduced (i.e., dimensionless) parameters $2D\tau/L_c^2$ and $n_P L_c^3$, which correspond to τ and C_P, respectively. As seen in parts a and b of Figure 7, the experimental data points are all on two master curves (straight lines) and the crossover concentration, C_G, is found independently of N as an inflection point between the two lines. This clearly indicates that the crossover behavior in the C_P dependence of τ and $\Delta\epsilon$ results from that of ξ given by eq 3 and 4. Then, it is concluded that the high-frequency dielectric relaxation in the dilute and semidilute regions is ascribable to the localized movement or fluctuation of the loosely bound counterions within the range of ξ in both the regions.

Figure 7c shows that the reduced parameter $\Delta\epsilon L_c^2/2D\tau$ corresponding to $\Delta\epsilon/\tau$ is proportional to $n_P L_c^3$ and

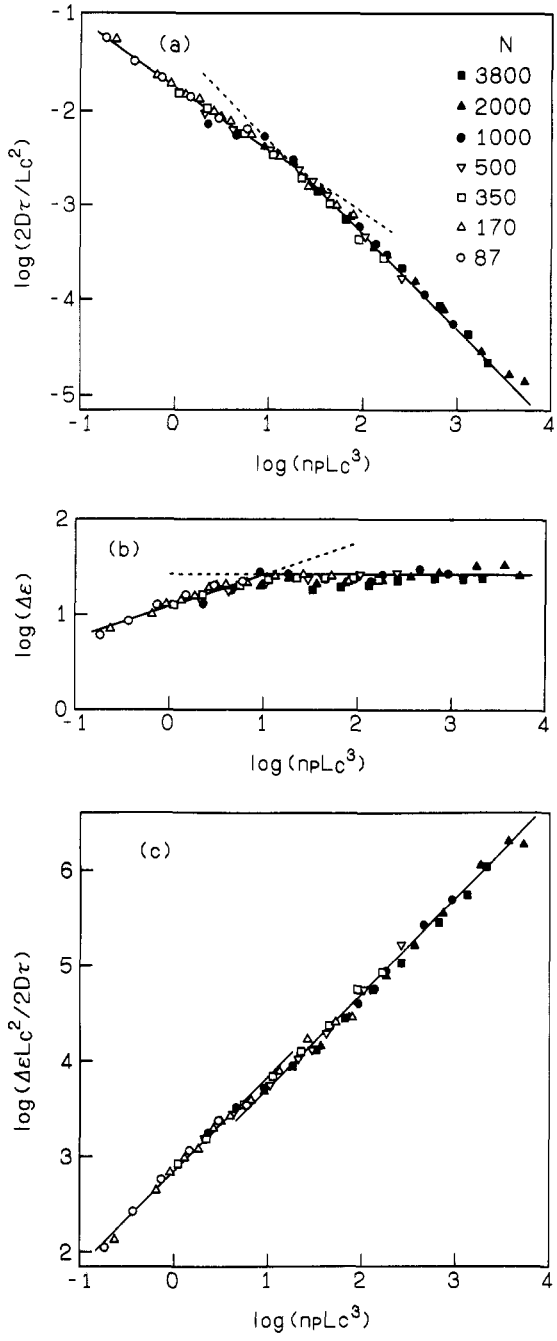

Figure 7. (a) Doubly logarithmic plot of $2D\tau/L_c^2$ against $n_pL_c^3$; the solid straight lines have a slope of −1 or −2/3. (b) Doubly logarithmic plot of $\Delta\epsilon$ against $n_pL_c^3$; the solid straight lines have a slope of 0 or 1/3. (c) Doubly logarithmic plot of $\Delta\epsilon L_c^2/2D\tau$ against $n_pL_c^3$; the straight lines have a slope of unity. In these figures, each symbol represents the sample difference as in Figure 3.

that the proportional constant $\Delta\epsilon/2D\tau n_pL_c$ is larger in the dilute region than it is in the semidilute one. This can be interpreted as follows: in the dilute region, the movement of the loosely bound counterions in all three directions contributes to the high-frequency relaxation while, in the semidilute region, only the motion in the two directions perpendicular to the polyion axis contributes. Thus, even if the number ratio of the loosely bound counterions to the total ones is the same in both regions, $\Delta\epsilon/2D\tau n_pL_c$ in the dilute region should be 1.5 times as large as it is in the semidilute region. This ratio roughly agrees with the experimental value 1.3 obtained from the limiting values of the dilute and semidilute regions in Figure 7c, which indicates that nearly the same ratio of the loosely bound counterions to the total ones contributes to the high-frequency relaxation in both regions.

The experimental result[25] by the small-angle X-ray scattering (SAXS) has revealed the correlation peak corresponding to ξ in the wavelength dependence of the scattering intensity and the crossover behavior for the C_P dependence of the peak in the dilute and semidilute regions of the NaPSS solution. The existence of the correlation peak, which is understood in terms of the correlation hole concept,[26] means the narrow distribution of the interpolyion distance resulting from the electrostatic (Coulombic) repulsion between polyions. The present result that the high-frequency relaxation process is close to Debye type may be ascribed to this narrow distribution.

The value of n_P corresponding to the crossover concentration, C_G, is estimated from parts a and b of Figure 7 as

$$n_pL_c^3 \simeq 10 \tag{15}$$

which is almost independent of N and in a good agreement with the observed results by SAXS.[25] These results mean that dielectric relaxation spectroscopy is useful for obtaining information about ξ over a wide C_P range from the dilute region to the semidilute, since the high-frequency relaxation process is closely related to ξ and has a sufficiently large dielectric increment to be detected even in a very dilute region.

In conclusion, the dielectric relaxation spectroscopy for the polyion solutions has revealed that the crossover behavior of the high-frequency relaxation in the dilute and semidilute regions is well explained in terms of the correlation length, ξ, which has a different C_P dependence in both the regions, and that the molecular mechanism of the high-frequency relaxation is ascribed to the localized movement or fluctuation of the loosely bound counterions within the range of ξ, namely, the average distance between polyions. The dielectric relaxation spectroscopy can afford the information not only on the profile of Coulombic potential in which the bound counterions fluctuates but also on ξ over a wide range of C_P from the dilute to the semidilute.

Acknowledgment. This work was partly supported by the Grant-in-Aid for Scientific Research from the Ministry of Education, Science and Culture of Japan.

Registry No. NaPSS, 9080-79-9.

References and Notes

(1) Oosawa, F. *Polyelectrolytes*; Marcel Dekker: New York, 1971.
(2) Manning, G. S. *Q. Rev. Biophys.* **1978**, *11*, 179.
(3) Mandel, M.; Odijk, T. *Ann. Rev. Phys. Chem.* **1984**, *35*, 75.
(4) Mandel, M.; Jenard, A. *Trans. Faraday Soc.* **1963**, *59*, 2158; 2170.
(5) Minakata, A. *Biopolymers* **1972**, *11*, 1567.
(6) Minakata, A.; Imai, N.; Oosawa, F. Biopolymers **1972**, *11*, 347.
(7) Muller, G.; van der Touw, F.; Zwoble, S.; Mandel, M. *Biophys. Chem.* **1974**, *2*, 242.
(8) Sakamoto, M.; Kanda, H.; Hayakawa, R.; Wada, Y. *Biopolymers* **1976**, *15*, 879.
(9) Sakamoto, M.; Hayakawa, R.; Wada, Y. *Biopolymers* **1978**, *17*, 1507; **1979**, *18*, 2769; **1980**, *19*, 1039.
(10) Minakata, A.; Imai, N. *Biopolymers* **1972**, *11*, 329.
(11) van der Touw, F.; Mandel, M. *Biophys. Chem.* **1974**, *2*, 218, 231.
(12) Odijk, T. *Macromolecules* **1979**, *12*, 688.
(13) Minakata, A. *Ann. N.Y. Acad. Sci.* **1977**, *303*, 107.
(14) Imai, N.; Sasaki, S. *Biophys. Chem.* **1980**, *11*, 361.
(15) Hall, B.; Wennerstroem, H.; Piculell, L. *J. Phys. Chem.* **1984**, *88*, 2482.

(16) Cametti, C.; Di Biasio, A. *Macromolecules* **1987**, *20*, 1579.
(17) Ookubo, N.; Hirai, Y.; Ito, K.; Hayakawa, R. *Macromolecules* **1989**, *22*, 1359.
(18) Hayakawa, R.; Kanda, K.; Sakamoto, M.; Wada, Y. *Jpn. J. Appl. Phys.* **1975**, *14*, 2039.
(19) Hayakawa, R.; Wada, Y. *IEE Conf. Publ.* **1979**, *177*, 396.
(20) Umemura, S.; Hayakawa, R.; Wada, Y. *Biophys. Chem.* **1980**, *11*, 317.
(21) Havriliak, S.; Negami, S. *J. Polym. Sci.* **1966**, *C14*, 99.
(22) Katchalsky, A. *Pure Appl. Chem.* **1971**, *26*, 327.
(23) Guéron, M.; Weisbuch, G. *J. Phys. Chem.* **1979**, *83*, 1991.
(24) Guéron, M.; Weisbuch, G. *Biopolymers* **1980**, *19*, 353.
(25) Kaji, K.; Urakawa, H.; Kanaya, T.; Kitamaru, R. *J. Phys.* (*Les Ulis, Fr.*) **1988**, *49*, 993.
(26) Hayter, J.; Jannink, G.; Brochard-Wyart, F.; de Gennes, P.-G. *J. Phys., Lett.* **1980**, *41*, L-451.

Studies on Probe Diffusion and Accessibility in Amylose Gels

V. M. Leloup and P. Colonna

INRA BP 527, Rue de la Geraudière, 44026 NANTES, Cedex 03, France

S. G. Ring*

AFRC Institute of Food Research, Norwich Laboratory, Colney Lane, Norwich NR4 7UA, U.K. *Received December 5, 1988; Revised Manuscript Received July 12, 1989*

ABSTRACT: The concentration dependence of the porosity of aqueous amylose gels was determined using two complementary experimental approaches. In the first, the volume of the gel accessible to probe species was investigated and an average pore size calculated. The probe species included globular proteins, flexible coil polysaccharides, and latex spheres. In the second, the effect of the gel network on retarding the diffusion of a globular protein (bovine serum albumin) was examined. The retardation in diffusion was considered to be due to hydrodynamic screening. The observed concentration dependence of screening length was compared to that predicted by recent theoretical approaches.

Introduction

The diffusion of solutes through porous media, including polymeric matrices, has many practical applications including the controlled release of pharmaceuticals and agrochemicals.[1-3] Usually the solute is a low molecular weight species. The rate of release may be manipulated by controlling the extent and rate of swelling of the matrix and hence the pore size. It is also of interest to study the diffusion of macromolecular species in similar matrices. In some applications, the controlled release of enzymes may be an objective; in others, enzymes may be used to degrade the polymer matrix which contains the active ingredient. In either case, in order to manipulate the rate of release, it is necessary to understand the relationship between the pore size of the matrix and the diffusion rate and accessibility of the macromolecule.[2,4]

The study of the diffusion of probe species in semidilute macromolecular solutions and gels is a topic of continuing research.[5-9] An early theoretical approach modeled the polymer solution or gel as a random collection of fixed rigid rods. A diffusive step was not allowed if it would have involved collision with obstacle.[10] More recently, hydrodynamic screening has been thought to be a more appropriate description of the physical process responsible for the retardation of diffusion.[11-13] In these approaches, semidilute solutions were considered as a three-dimensional fishnet characterized by an average mesh size, ξ, which corresponds to the distance between two entanglement points. The hydrodynamic behavior of a probe molecule depends strongly on the ratio of the probe hydrodynamic radius, R_H, to the mesh size, ξ. When $R_H \ll \xi$, the matrix appears as a continuum, and the Stokes-Einstein relationship

$$D = k_B T / 6\pi\eta R_H \quad (1)$$

may be used to describe the diffusion process, where D is the diffusion coefficient of the probe, k_B and T have their usual meanings, and η is the macroscopic viscosity of the polymer solution. When R_H and ξ are of comparable scale, the hydrodynamic behavior of the probe molecule diverges from eq 1 and shows a strong dependence upon polymer concentration. There has been recent interest, both theoretical[14,15] and experimental,[5,6,8,9] on the influence of polymer concentration on mesh size and on the diffusion of probe particles in polymer networks. There have been fewer studies on probe diffusion in gel matrices, although the diffusion of dextrans in agarose gels has recently been examined by quasi elastic light scattering (QELS).[16] Polymer gels are usually pictured as infinite three-dimensional networks, within which the polymer molecules mobility is rather small. In this case, when $R_H \gg \xi$, the probe particle is totally excluded from the gel. Usually the mesh size varies over a quite wide range, and the gel may be more or less accessible to probe species of a varying size range.

The study of the effect of networks on diffusion and accessibility of macromolecular probes is important to understanding factors that might limit the enzymic degradation of porous biopolymeric materials and is thus relevant to biotransformations, nutrition, and some controlled release applications. In this study the porosity of a gel network of the starch polymer amylose was examined.

Amylose is an essentially linear polysaccharide composed of α-(1-4)-linked D-glucose units. Concentrated aqueous solutions of amylose form turbid gels on cooling to room temperature.[17,18] The turbidity of the gels

0024-9297/90/2223-0862$02.50/0